A Project Report

On

PERFORMANCE EVALUATION OF MILLIMETER-WAVE MASSIVE MU-MIMO FOR HIGH-EFFICIENCY WIRELESS COMMUNICATIONS IN UNDERGROUND MINES

Submitted in partial fulfillment for the award of the degree of

Bachelor of Technology

in

Electronics and Communications Engineering

by

G.RUPAKIRAN	22F65A0420
G.REDDY PRASANNA	22F65A0419
M.SAINATH NAIK	21F61A04H4
S.ANIS AHAMMAD	21F61A04I6
B.SIVASANKAR	21F61A04K3

Under the esteemed guidance of

Mr. K. SANTHOSH KUMAR

Assistant Proffessor,Department of ECE

Department of Electronics and Communications Engineering

SIDDHARTH INSTITUTE OF ENGINEERING & TECHNOLOGY

(AUTONOMOUS)

(Approved by AICTE & Affiliated to JNTUA, Ananthapuramu)
(Accredited by NBA for Civil, EEE, ECE, MECH and CSE, New Delhi)
(Accredited by NAAC with 'A+' Grade, an ISO 9001:2008 Certified Institution)
Siddharth Nagar, Narayanavanam road, Puttur-517583, A.P

2025

SIDDHARTH INSTITUTE OF ENGINEERING & TECHNOLOGY

(AUTONOMOUS)

(Approved by AICTE & Affiliated to JNTUA, Ananthapuramu)
(Accredited by NBA for Civil, EEE, ECE, MECH and CSE, New Delhi)
(Accredited by NAAC with 'A+' Grade, an ISO 9001:2008 Certified Institution)
Siddharth Nagar, Narayanavanam road, Puttur-517583, A.P
DEPARTMENT OF ELECTRONICS AND COMMUNICATIONS ENGINEERING

CERTIFICATE

*This is to certify that the Project entitled "***PERFORMANCE EVALUATION OF MILLIMETER-WAVE MASSIVE MU-MIMO FOR HIGH-EFFICIENCY WIRELESS COMMUNICATIONS IN UNDERGROUND MINES***" that is being submitted by*

G.RUPAKIRAN	**22F65A0420**
G.REDDY PRASANNA	**22F65A0419**
M.SAINATH NAIK	**21F61A04H4**
S.ANIS AHAMMAD	**21F61A04I6**
B.SIVASANKAR	**21F61A04K3**

is in partial fulfillment of the requirements for the award of BACHELOR OF *TECHNOLOGY in* ELECTRONICS AND COMMUNICATIONS ENGINEERING *to* JNTUA , ANANTHAPURAMU. *The results embodied in this Project report have not been submitted to any other University or Institute for the award of any degree.*

Internal Guide

Mr. K. SANTHOSH KUMAR
Assistant Proffessor,
Department of ECE,
SIETK.

Head of the Department

Dr. P. RATNA KAMALA, MTech., Ph.D.
Head of the Department,
Department of ECE,
SIETK.

Submitted for the project viva-voce examination held on _____

Internal Examiner **External Examiner**

Acknowledgement

*We wish to express our profound and sincere gratitude to **Mr. K Santhosh Kumar**, Assistant Professor, Department of ECE, **Siddharth Institute of Engineering & Technology, Puttur**, who guided us into the intricacies of this project with utmost clarity.*

*We would also like to extend our gratitude to **Dr. P Ratna Kamala**, Head of the Department of Electronics and Communications Engineering for her encouragement and for providing the facilities to carry out the work in a successful manner.*

*We are thankful to **Dr. K. Chandrasekhar Reddy**, Principal for his encouragement and support.*

*We wish to express our sincere thanks to **Dr. K. Indira Veni, Vice-Chairman,** and **Dr. K. Ashok Raju, Chairman** of Siddharth Group of Institutions, Puttur, for providing ample facilities to complete the project work.*

We would also like to thank all the faculty and staff of the Electronics and Communications Engineering Department, for helping us to complete the project work.

Very importantly, we would like to place on record our profound indebtedness to our parents and families for their substantial moral support and encouragement given throughout our study

TABLE OF CONTENTS

ABSTRACT

This paper examines the performance of a large multiuser multiple-input and multiple-output (MU-MIMO) millimetre wave (mmWave) channel in an underground mine. Based on channel measurements made at 28 GHz with a base station of 128 virtual antenna components supporting several customers, the study was carried out. Large-scale path loss, temporal dispersion, coherence bandwidth, and sum-rate capacity are among the channel parameters that are reported and assessed. According to the findings, the multislope path loss model performs better when it comes to accurately predicting path loss across different propagation segments inside the mining gallery. Ninety percent of the root-mean-square (rms) delay spreads are less than 4 ns, according to the time dispersion analysis, which indicates that the underground mine channel does not significantly increase time dispersion. Furthermore, it was discovered that the propagation distance has no bearing on the rms delay spread. The potential of using massive MIMO technology to increase the channel's spectral efficiency is highlighted by the sum-rate capacity study. According to the investigation, the capacity can reach up to 33.54 bit/s/Hz with eight active users. Rich-scattering and irregular topology are two characteristics of the deep mine environment. The results of this article provide important insights into these propagation aspects.

Keywords: 5G, 28 GHz, Channel Capacity, Channel Measurements, Massive Multiuser Multiple Input and Multiple Output (MU-MIMO), Millimeter-Wave (mmWave), Path Loss, Root- Mean-Square (RMS) Delay Spread, Underground Mine, 128 Base Station Antennas.

LIST OF FIGURES

SYMBOLS & ABBREVIATIONS

ACRONYM	ABBREVIATION
5G	Fifth Generation (Wireless Technology)
AI	Artificial Intelligence
AP	Access Point
API	Application Programming Interface
AWGN	Additive White Gaussian Noise
BD	Block Diagonalization
BER	Bit Error Rate
BS	Base Station
CIR	Channel Impulse Response
CTF	Channel Transfer Function
DL	Downlink
dBi	Decibels relative to isotropic radiator
dBm	Decibels relative to 1 milliwatt
EMF	Electromagnetic Field
FFT	Fast Fourier Transform
GPU	Graphics Processing Unit
HDD	Hard Disk Drive
HDL	Hardware Description Language
ID	Interference Detection
IoT	Internet of Things
IW	Interference Whitening
LOS	Line of Sight
MATLAB	Matrix Laboratory
MIMO	Multiple Input Multiple Output
mm wave	Millimeter
ML	Machine Learning
NLOS	Non Line of Sight
OBD	Optimized Block Diagonalization
OFDM	Orthogonal Frequency Division Multiplexing

OFDMA	Orthogonal Frequency Division Multiple Access
PC	Personal Computer
PLE	Path Loss Exponent
PLC	Power Line Communication
RF	Radio Frequency
RFoF	Radio Frequency over Fiber
RIS	Reconfigurable Intelligent Surfaces
RMS	Root Mean Square
Rx	Receiver
SISO	Single Input Single Output
SNR	Signal-to-Noise Ratio
Tx	Transmitter
URA	Uniform Rectangular Array
USB	Universal Serial Bus
VNA	Vector Network Analyzer
ZF	Zero Forcing

CHAPTER 1
INTRODUCTION

1.1 Introduction to Wireless Communication Challenges

As the use of broadband access services by various handheld devices, including laptops, tablets, and smartphones, has grown, so has the importance of boosting transmission speed in a constrained frequency range in wireless communications. Many technologies have been able to reach higher transmission rates, and research is still being done to determine how to increase transmission rates even further. Multiple-input multiple- output (MIMO) communication has been regarded as a crucial technology for reaching high data rates for decades. Multiuser (MU)-MIMO antenna technology has been researched and used in a variety of consumer goods recently. IEEE 802.11ac, a widely utilized wireless local area network standard in MU-MIMO downlink (DL) systems, serves as the representative standard for such products. Attracting a lot of attention are standardization developments like IEEE 802.11n, whereas IEEE 802.11ac targets for a transmission speed of at least 1 Gbps DL MU-MIMO transmission technology in the 5 GHz band has been proposed for IEEE 802.11ac. With this technology, the physical layer's maximum transfer rate is roughly 7 Gbps.MINE 4.0 or smart mine is the name that is generally given to the mine which adopts the characteristics specific to the fourth industrial revolution (Industry 4.0)

1.2 Mining 4.0 and Smart Mine Initiatives

To improve safety and productivity, mining companies are rapidly deploying new tools and technologies including telemetry, wireless sensors, and remote mining. Mining 4.0 makes use of technologies such as the fifth- generation mobile network (5G), Internet of Things (IoT) sensing, artificial intelligence (AI), and machine learning .

Nowadays, most of mining companies are planning to invest in wireless infrastructure and most of them named the private (nonpublic) 5G networks as their priority. It is anticipated to provide ultrahigh data rates in the multi-Gb/s range, along with submillisecond latency. This will enable operation of autonomous vehicles, real-time status tracking of equipment and miners, remote diagnostic and maintenance, and facilitate the connection of hundreds of thousands of IoT sensors and devices, both on surface and underground.

1.3 Unique Challenges in Underground Mine Communications

Compared to conventional residential, commercial, and industrial indoor environments, establishing fully flexible and high-speed reliable networks face unique propagation challenges in underground mine which require innovative solutions. Underground mining environments are known for having walls with extremely rough surfaces, confined space, and

an expanding network of tunnels and galleries, which make network planning, and deployment more challenging Therefore, a precise channel characterization based on realistic measurements is necessary to design an efficient 5G wireless communication network for underground mines.

1.4 mm Wave and Massive MIMO Integration

The implementation of industrial 5G systems will require significant improvements in terms of transmission bandwidth, which can be achieved by utilizing new bands at higher frequencies.Hence, mmWave spectrum is one key enabling solution for meeting the enormous increase in channel capacity demand.However, millimeter-wave (mmWave) channels are strongly sensitive to environment dimensions, presence of physical obstacles and scatterers These higher frequencies often experience significant path loss and require a clear line of sight (LOS) between the transmitter and receiver. Therefore, massive multipleinput and multipleoutput (MIMO) techniques have the capability to address these challenges and greatly improve the spectral efficiency .

The combination of mmWave and massive MIMO is expected to drastically enhance the wireless network performance, by bringing together the huge available mmWave bandwidth and the expected gain of massive MIMO arrays, making them the best solutions for 5G systems,While the challenges confronting mmWave and massive MIMO applications in underground mine environments are substantial, including high signal attenuation, the complex 3-D nature of mines with limited direct links, multipath interference undermining signal integrity, potential signal blockage due to machinery and infrastructure, the precision required for beamforming alignment, and potential interference from neighboring communication systems. Nevertheless, the adoption of mmWave and massive MIMO technologies in underground mine wireless communications offers a multitude of advantages. Beyond the high data rates and low latency benefits, these technologies excel in enhancing signal quality through precise signal direction, effectively addressing multipath effects and interference.

Moreover, the utilization of directional beamforming optimizes coverage over extended tunnel distances, minimizing signal attenuation compared to omnidirectional propagation.
The adaptability of mmWave and Massive MIMO systems to the tunnel's unique geometry further helps in optimizing coverage while mitigating signal blockage challenges. By reducing interference through directional propagation and beamforming, these technologies ensure more reliable and consistent communication links.

1.5 MU-MIMO Systems and Interference Issues

Unlike conventional MIMO systems, in MU-MIMO systems, multiple users can communicate simultaneously using a single access point (AP). In other words, in a DL setting, a signal that an AP sends to a specific user also reaches other users. Users simultaneously receive the targeted signal and the so-called interfering signals. These signals are known as interfering signals. These conflicting signals consequently lower performance.

1.6 Precoding Techniques for Interference Mitigation

As a result, the majority of DL MU-MIMO systems use precoding technology in the AP in an effort to address the interference issue . In order to prevent interference signals from affecting any user, the AP pre-codes the channel by multiplying a precoding matrix on it beforehand. For instance, in the representative zero- forcing beamforming technology, each user and the AP are made up of a MIMO system, and theoretically, an interfering signal can be zero the entire MU-MIMO system is divided into MIMO However, in real-world environments, errors, referred to as practical errors, inevitably occur due to errors in channel estimation and incomplete calculation. This practical errors result in an incomplete precoding matrix; thus, some users will still receive interfering signals. Compared to the desired signal, the interference signal is relatively small; however, these signals are enough to affect system performance Therefore, an interference-aware receiver is required.

1.7 Practical Challenges and Solutions

There have been several suggestions made for DL MU-MIMO systems to reduce inter-user interference. Interference whitening (IW) and interference detection (ID) are two representative approaches that these techniques can be divided into. IW is less computationally complex than ID since it interprets interference as Gaussian noise but it is insufficient for strong interference. Numerous interference rejection combiners and their extensions have explored the IW method .Even yet, they are still unable to operate at a high level when there is significant interference. To reduce interference, ID, on the other hand, recognises both desired signals and interfering signals .ID has a high computational complexity but can attain great performance, which is considered optimum. There were multiple approaches to simplify the existing MIMO decoder algorithms. While this method is far more sophisticated than IW, it can reduce complexity when compared to identity.

Therefore, ID is not taken into account for actual implementation. DL MU- MIMO systems, both present and prospective, have a problem with the performance of IW in high interference environments, as was previously mentioned. In order to achieve an appropriate hardware implementation, we provide in this study a symbol detector architecture with an interference mitigation method appropriate for DL MU-MIMO systems. Numerous studies on the hardware implementation of MIMO detection algorithms have been published to date .

Despite their ubiquitous use, no studies have attempted to create implementations for DL MU-MIMO systems. Consequently, we concentrate on enhancing current MIMO detectors for DL MU-MIMO systems by fusing them with an algorithm for mitigating interference. The goal of this procedure is to reduce costs in relation to compatibility with current
MIMO detectors which we expect to simplify the adaptation of the MIMO detectors to DL MUMIMO systems.

1.8 Block Diagonalization (BD) in MU-MIMO

Block Diagonalization (BD) is a linear precoding technique used in multiuser multipleinput multiple-output (MU-MIMO) systems to mitigate interference between users and optimize system performance. BD transforms the multi-user interference into a block diagonal form, allowing each user to be treated as if they were in a single-user scenario. This method is particularly useful in large-scale MIMO systems where multiple users share the same frequency resources.

1.MU-MIMO Systems:

In MU-MIMO systems, a base station (BS) equipped with multiple antennas serves multiple users simultaneously. The channel matrix for each user can be complex and may result in significant interference between users.

2.Interference Mitigation:

The main challenge in MU-MIMO systems is to manage interference from other users.
Traditional techniques like Zero Forcing (ZF) and Minimum Mean Square Error (MMSE)

3.Block Diagonalization (BD):

BD aims to diagonalize the overall channel matrix in such a way that the interference between different users is minimized. This results in a block diagonal form of the matrix, where each block corresponds to a user's channel matrix.

4.Optimized Block Diagonalization (OBD):

OBD extends BD by incorporating optimization techniques to enhance performance. The goal of OBD is to improve upon the standard BD approach by optimizing the precoder design and channel matrix transformation.

CHAPTER 2
LITERATURE REVIEW

R. Flamini et al., "Toward a heterogeneous smart electromagnetic environment for millimeter-wave communications: An industrial view-point," IEEE Trans. Antennas Propag., vol. 70, no. 10, pp. 8898–8910, Oct. 2022.: Fifth generation (5G) and beyond communication systems open the door to millimeter Wave (mmWave) frequency bands to leverage the extremely large operating bandwidths and deliver unprecedented network capacity. These frequency bands are affected by high propagation losses that severely limit the achievable coverage. The simplest way to address this problem would be to increase the number of installed mmWave base stations (BSs), at the same time augmenting the overall network cost, power consumption and ElectroMagnetic Field (EMF) levels. As alternative direction, here we propose to complement the macro-layer of mmWave BSs with a heterogeneous deployment of Smart Electromagnetic (Smart EM) Entities - namely IAB nodes, Smart Repeaters, Reconfigurable Intelligent Surfaces (RISs) and passive surfaces - that is judiciously planned to minimize the total installation costs while at the same time optimizing the network spectral efficiency. Initial network planning results underline the effectiveness of the proposed approach. The available technologies and the key research directions for achieving this view are thoroughly discussed by accounting for issues ranging from system-level design to the development of new materials.

Summary: Studied on the heterogeneous smart electromagnetic environment for millimeter-Wave communications as an industrial view-point.

O. Kolade and L. Cheng, "Markov model characterization of a multicarrier narrowband powerline channel with memory in an underground mining environment," IEEE Access, vol. 9, pp. 59085–59092, 2021: The error distribution of multicarrier modulation in a narrowband powerline communication (PLC) channel with memory is presented for an underground mining environment. In the environment, the noise in the PLC channel originates from the mains switchboard and a blast control unit, connected to the powerline link. Using the error vectors measured from the channel, the memory channel model is obtained by training the measured data using a hidden Markov model and the Fritchman model for channel state classification. The channel with memory is modeled by considering the state transition measured data using a hidden Markov model and the Fritchman model for channel state classification. The channel with memory is modeled by considering the state transition probabilities between the current state and one previous state of the channel. The measured and modeled data are then compared in order to determine the suitability of the derived models. Using the error-free run distribution and probabilities of error of the modeled data,

the modeled data match the measured data, validating the suitability of the derived models for an underground mining environment.

Summary: Studied about Markov model characterization of a multicarrier narrowband power line channel with memory in an underground mining environment.

S. M. Riurean, M. Leba, and A. C. Ionica, "Conventional and advanced technologies for wireless transmission in underground mine," in Application of Visible Light Wireless Communication in Underground Mine. Cham, Switzerland: Springer, 2021, pp. 41–125:

Mining activity is one of the most difficult and dangerous in the world. Miners' security and safety have always been a main concern for the mining companies besides the high productivity and economic growth.

Summary: Studied about the conventional and advanced technologies for wireless transmission in underground mine.

S. A. M. Tariq, C. L. Despins, S. Affes, and C. Nerguizian, "Angular dispersion of a scattered underground wireless channel at 60 GHz," IEEE Access, vol. 8, pp. 67572– 67580, 2020: The 60 GHz frequency band is identified as a suitable band for Gbps speed wireless communication in an Underground mine due to its high antenna directivity and high signal attenuation. However, the rough mine surface and the 5 mm wavelength may produce rich scattering phenomenon of multipath signals. To characterize the channel and more insight into the scattering, the angular dispersion measurements are conducted in different mine gallery depths and dimensions. The scattering is analyzed by the angle of arrivals of the incoming paths at the receiver, which is characterized by the statistical parameters of the multipath shape factors. The results of the multipath shape factor are explained and show that at around 3 m link distance, the incoming paths are mostly in two or three directions within a resolution angle of around between ±30° and ±40°. The statistical distribution of the multipath angle of arrivals follows a Gaussian probability distribution. The results also show that the angular spreads of multipath are proportional to the gallery dimensions and inversely proportional to the link distances.

Summary: Studied about angular dispersion of a scattered underground wireless channel at 60 GHz.

C.Wang, W. Ji, G. Zheng, and A. Saleem, "Analysis of propagation characteristics for various subway tunnel scenarios at 28 GHz," Int. J. Antennas Propag., vol. 2021, pp. 1–16, Sep. 2021. In order to meet the higher data transmission rate requirements of subway communication services, the millimeter wave (mm Wave) broadband communication is considered as a potential solution in 5G technology. Based on the channel measurement data in subway tunnels, this paper uses ray-tracing (RT) simulation to predict the propagation characteristics

of the 28 GHz millimeter wave frequency band in different tunnel scenarios. A large number of simulations based on ray-tracing software have been carried out for tunnel models with different bending radiuses and different slopes, and we further compared the simulation results with the real time measurement data of various subway tunnels. The largescale and small-scale propagation characteristics of the channel, such as path loss (PL), root mean square delay spread (RMS-DS), and angle spread (AS), for different tunnel scenarios are analyzed, and it was found that the tunnel with a greater slope causes larger path loss and root mean square delay spread. Furthermore, in the curved tunnel, the angle spread of the azimuth angle is larger than that in a straight tunnel. The proposed results can provide a reference for the design of future 5G communication systems in subway tunnels.

Summary: Studied about the analysis of propagation characteristics for various subway tunnel scenarios at 28 GHz.

CHAPTER 3
EXISTING METHOD

To characterize the mmWave Massive MU-MIMO channel in an underground mine, wideband measurements were conducted at 28 GHz using frequency-domain channel sounding. The 28 GHz band is among the most important bands in mmWave communication according to the regulations of 3GPP and ITU WRC-15. Recently, the 3GPP band n257 (27.5–28.35 GHz) was adopted to support the millimeter-wave spectrum in Canada and USA .It is worth mentioning that this potential candidate band is still unexplored in underground mine environments.

3.1 Underground Mine Description

The measurement campaign was performed in the Old Lamaque mine which is a former gold mine located in Val D'or, QC, Canada. An underground gallery at a depth of 91 m was exploited to carry out propagation measurements. This gallery has a downward slope of approximately 20% over 50 m serving as a connecting tunnel between the auditorium and a lower level. Beyond this point, the tunnel extends horizontally for 150 m with several curves along the way. The gallery consists of an arched ceiling tunnel with a mean width of 3.8 m and a mean height of 2.8 m. The walls are very rough and consist of sharp edges. The humidity level can reach 100% and the temperature is about 8 ∘C. The gallery is equipped with a roof bolting system that consists of metallic rods and nets. Fig. shows the plan layout of the mining gallery.

3.2 Experimental Setup

The experimental setup used in this measurement campaign is illustrated in Fig. 2. The measurement system is base.

on the frequency domain channel sounding method. The system mainly consisted of a vector network analyzer (VNA) Anritsu MS4647A, that operates from 10 MHz to 70 GHz, to measure the forward transmission coefficient S21(f) of the wireless channel, equivalent to the complex channel transfer function (CTF) H(f) . In addition, the Anritsu MS4647A offers a time domain option by transforming the frequency response, using the chirp z inverse fast Fourier transform, into the time domain which is equivalent to the channel impulse response (CIR) h(t) Omnidirectional antenna (gain of 1 dBi) was used at the receiver (Rx) side during the measurement campaigns. For the transmitter (Tx) side, a waveguide horn antenna (gain of 20 dBi) was employed due to its capability of directing a significant portion of the transmitted power toward the mine gallery, thereby.

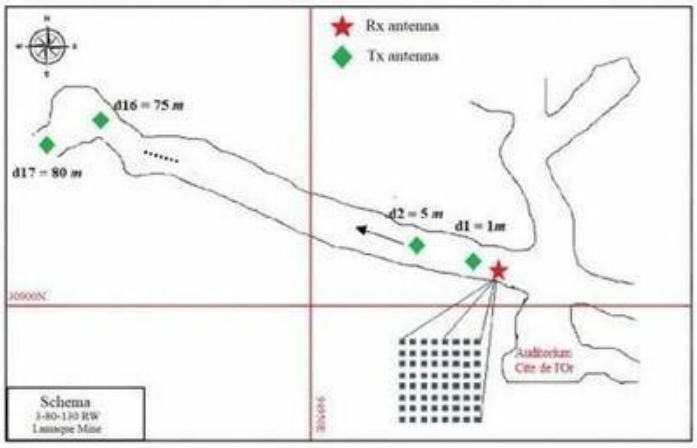

Fig 1: Mining Gallery Plan Layout

The main drawback of using channel sounder-based VNA is the limitation of range and mobility due to the high attenuation by RF cables, especially at mmWave frequencies. To address this issue, a broadband RFoF link (by Optilab) is considered to connect the Tx antenna to the VNA. This part of the setup consists of a high-performance lightwave transmitter module (LTA-40) connected to a bandwidth PIN receiver module (PD- 40-M- dc) through a single-mode fiber, operating from dc to 40 GHz.

Hence, the low attenuation of the optical fiber (1.5 dB/km) allows for improving the dynamic range of the sounder which could extend the measurement range from few meters to several hundreds of meters. In addition, an amplifier (gain of 50 dB) is also connected to the Tx antenna to compensate for the losses introduced by the RFoF link before transmission .The Rx antenna has been mounted on a 3-D motion control positioning system from Velmex, Inc., which allows vertical planar scanning to form a virtual uniform rectangular array (URA). The 3-D positioning system and the VNA were both remotely controlled using a personal computer (PC) via serial cables (RS 232 and USB type B). A developed LabVIEW application was also used to simultaneously control the movement of the 3-D positioning system and to perform real-time data acquisition from the VNA.

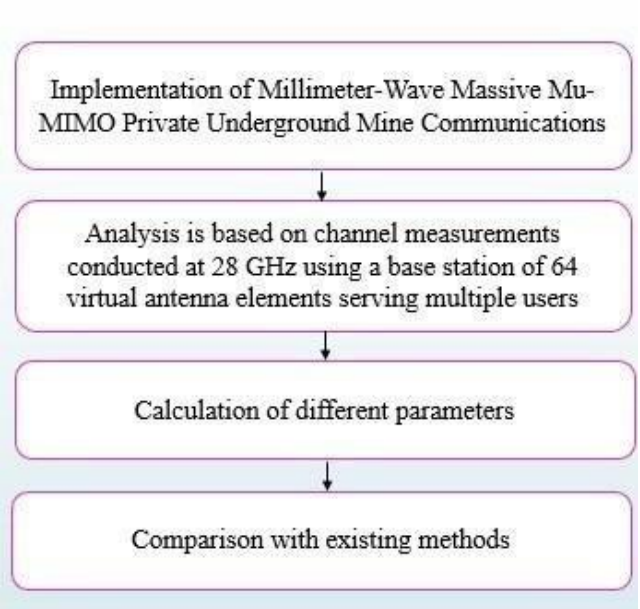

Fig 2: Flow of Existing Method

3.3 Measurement Procedure

The maximum RF transmit power was fixed at 6 dBm over the 800 MHz bandwidth. The number of sweep points was set to 1201 which corresponds to a maximum excess delay of 1.5 μs. Since the VNA takes time to sweep over the measured frequency bands, there were no moving people or objects in the gallery, leading to a static channel. To emulate an uplink massive MU-MIMO system, the Rx subsystem which is considered as a base station (BS), was placed close to the left side wall of the gallery at a height of 1.7 m to form a virtual URA of 64 elements uniformly spaced by $\lambda/2$ and perpendicular to the gallery wall. At the Tx side, the horn antenna was fixed on a tripod with a height of 1.6 m to emulate an active user equipment (UE). A total of 17 different locations were predefined on the mine galley of which 12 of them are related to LOS links (Tx1–Tx13), and the rest are referred to nonline of sight (NLOS), as illustrated in Fig.

The Tx horn antenna was aligned (using laser beam tool) to the center of the Rx URA, for all locations, to achieve the maximum received power. For each Tx–Rx combination, the CTF and the CIR were recorded providing a total of 2176 measurements. Finally, Table I summarizes the main parameters regarding the measurement settings. It is worth mentioning that before the measurement campaign, the VNA is first calibrated using ShortOpenLoad-Thru (SOLT) technique to remove the effect of RF cables and other passive elements in the measurement system. The CTF $H(f)$ can be derived from the measured transmission parameter $S21(f)$ which can be expressed in the frequency domain as follows:

$$S_{21}(f) = H\,(f)\,H_{sys}\,(f)$$

where Hsys(f) is the transfer function of the Tx and Rx link. To measure the impact of the equipment (RFoF link, fiber, and amplifier), reference measurements at 1-m separation distance have been conducted in an anechoic chamber. The measured S21ref(f) parameter can be expressed as follows:

$$S_{21ref}(f) = H_{ref}(f)\,H_{sys}\,(f)$$

Then, the transfer function of the Tx and Rx link equipment can be determined as follows:

$$H_s(f) = \frac{S_{21r}(f)}{H_r(f)}$$

where Href(f) is the free space transfer function.

3.3.1 Path Loss Measurement

Path loss denotes the signal power loss in the propagation channel and is used to determine link budgets by evaluating the propagation loss between the transmitter and the receiver. As a result, the path loss values are frequency-dependent rather than antenna gain or transmitted power level. The local wideband path loss can be extracted from the measured CTF as follows

the path loss values are frequency-dependent rather than antenna gain or transmitted power level. The local wideband path loss can be extracted from the measured CTF as follows

$$\mathrm{PL} = \frac{1}{N_f}\sum_{k=1}^{N_f}|H(f_k)|^2$$

where Nf is the number of sweep points. According to the calibration mentioned above, the CTF can be expressed as follows:

$$H\,(f_k) = \frac{S_{21}(f_k)}{H_{sys}(f_k)}$$

Finally, the wideband path loss can be obtained using the following expression:

N_f

$$\mathrm{PL(dB)} = -10\log_{10}\left[\frac{1}{N_f}\sum_{k=1}^{N_f}\left|\frac{S_{21}(f_k)}{H_{sys}(f_k)}\right|^2\right]$$

3.3.2 Path Loss Modeling

Large-scale path loss models are important in designing communication systems .They are used to predict link budgets by estimating the attenuation over the distance of propagating signals. Among different types of large-scale channel models (empirical, stochastic, and deterministic), path loss models based on measurements offer a realistic insight into propagation characteristics .Thus, two potential path loss models (log-distance and multislope) have been considered in this study. The log-distance path loss model is widely used in wireless communications because it provides a simple and practical way to predict the received signal strength .Hence, the log-distance path loss model can be used to estimate the large-scale fading resulting from multimode propagation in the underground mine .This model is parametrized by PLE parameter n, and it is given by the following equation.

$$\mathrm{PL[dB]} = \mathrm{PL_0[dB]} + 10\,\mathrm{n}\log_{10}\left[\frac{d}{d_0}\right] + \chi_\sigma$$

where PL0 is the path loss at a reference distance d0 (generally taken as 1 m), d is the Tx–Rx separation distance in meters, and $\chi\sigma$ is a zero mean Gaussian random variable with a standard deviation σ in dB.

In fact, the propagation in the mine gallery is based on the hypothesis that propagation takes the form of waveguide transmission.Therefore, in the LOS scenario, the signal undergoes free space propagation in the near region. Then, a lower attenuation is shown after a particular distance known as the breakpoint distance dbp .At the end of the LOS segment, the signal encounters a higher attenuation in the NLOS segment between 60 and 80 m.

As a result, a multislope path loss model is proposed for a better modeling of the wave propagation in the underground mining gallery. In a typical indoor and outdoor environment, separate path loss models are used for LOS and NLOS scenarios. However, in tunnel propagation, a more effective approach is to combine these path loss models into a single multislope path loss model and .The multislope path loss model is given by PL[dB]

$$= \begin{cases} \mathrm{PL}_0 + 10n_1\log_{10}\left(\frac{d}{d_0}\right) + \chi_{\sigma_1}, & \text{for } d \le d_{\mathrm{bp}} \\ \mathrm{PL}_{\mathrm{bp}} + 10n_2\log_{10}\left(\frac{d}{d_{\mathrm{bp}}}\right) + \chi_{\sigma_2}, & \text{for } d_{\mathrm{bp}} \le d \le d_{\mathrm{LOS}} \\ \mathrm{PL}_{\mathrm{LOS}} + 10n_3\log_{10}\left(\frac{d}{d_{\mathrm{LOS}}}\right) + \chi_{\sigma_3}, & \text{for } d \ge d_{\mathrm{LOS}} \end{cases}$$

where PLbp is the path loss at the breakpoint distance dbp, PLLOS is the path loss at the maximum LOS distance (dLOS = 60 m), n1, n2 and n3 are the PLEs, χσ1 , χσ2 , 3 are χσ and zero mean Gaussian variables with standard deviation of σ1, σ2, and σ3, respectively.

CHAPTER 4
PROPOSED METHOD

To characterize the mmWave Massive MU-MIMO channel in an underground mine, wideband measurements were conducted at 28 GHz using frequency-domain channel sounding. The 28 GHz band is among the most important bands in mmWave communication according to the regulations of 3GPP and ITU WRC-15 [33]. Recently, the 3GPP band n257 (27.5–28.35 GHz) was adopted to support the millimeter-wave spectrum in Canada and USA [34]. It is worth mentioning that this potential candidate band is still unexplored in underground mine environments.

4.1 Underground Mine Description

The measurement campaign was performed in the Old Lamaque mine which is a former gold mine located in Val D'or, QC, Canada. An underground gallery at a depth of 91 m was exploited to carry out propagation measurements. This gallery has a downward slope of approximately 20% over 50 m serving as a connecting tunnel between the auditorium and a lower level. Beyond this point, the tunnel extends horizontally for 150 m with several curves along the way. The gallery consists of an arched ceiling tunnel with a mean width of 3.8 m and a mean height of 2.8 m. The walls are very rough and consist of sharp edges. The humidity level can reach 100% and the temperature is about 8 ∘C. The gallery is equipped with a roof bolting system that consists of metallic rods and nets. Fig. shows the plan layout of the mining gallery.

4.2 Experimental Setup

The experimental setup used in this measurement campaign is illustrated in Fig. 2. The measurement system is base.

on the frequency domain channel sounding method. The system mainly consisted of a vector network analyzer (VNA) Anritsu MS4647A, that operates from 10 MHz to 70 GHz, to measure the forward transmission coefficient S21(f) of the wireless channel, equivalent to the complex channel transfer function (CTF) H(f) [35].

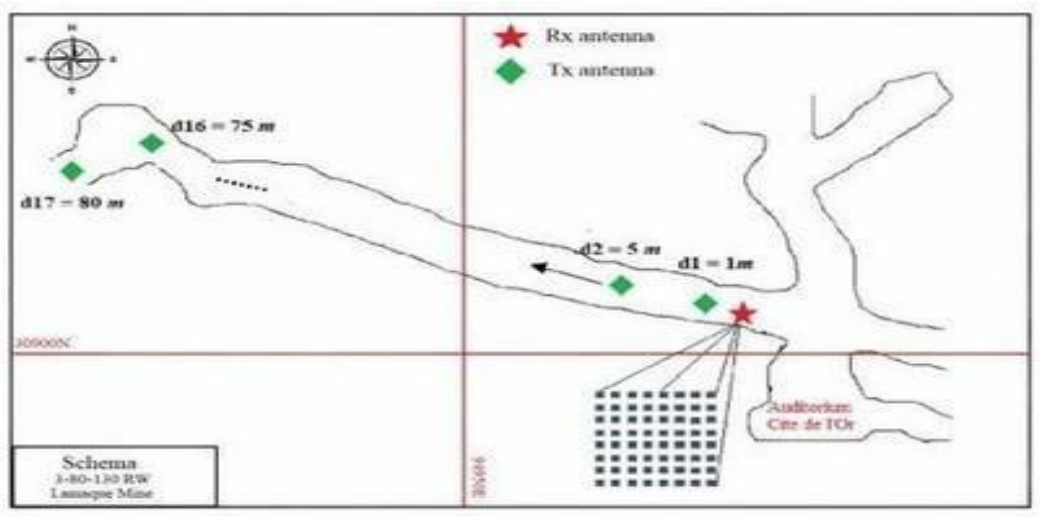

Fig 3: Mining Gallery Plan Layout

In addition, the Anritsu MS4647A offers a time domain option by transforming the frequency response, using the chirp z inverse fast Fourier transform, into the time domain which is equivalent to the channel impulse response (CIR) h(t) Omnidirectional antenna (gain of 1 dBi) was used at the receiver (Rx) side during the measurement campaigns. For the transmitter (Tx) side, a waveguide horn antenna (gain of 20 dBi) was employed due to its capability of directing a significant portion of the transmitted power toward the mine gallery, thereby enhancing the waveguide effect.

The main drawback of using channel sounder-based VNA is the limitation of range and mobility due to the high attenuation by RF cables, especially at mmWave frequencies. To address this issue, a broadband RFoF link (by Optilab) is considered to connect the Tx antenna to the VNA. This part of the setup consists of a highperformance lightwave transmitter module (LTA-40) connected to a bandwidth PIN receiver module (PD-40-M- dc) through a single-mode fiber, operating from dc to 40 GHz. Hence, the low attenuation of the optical fiber (1.5 dB/km) allows for improving the dynamic range of the sounder which could extend the measurement range from few meters to several hundreds of meters. In addition, an amplifier (gain of 50 dB) is also connected to the Tx antenna to compensate for the losses introduced by the RFoF link before transmission The Rx antenna has been mounted on a 3-D motion control positioning system from Velmex, Inc.

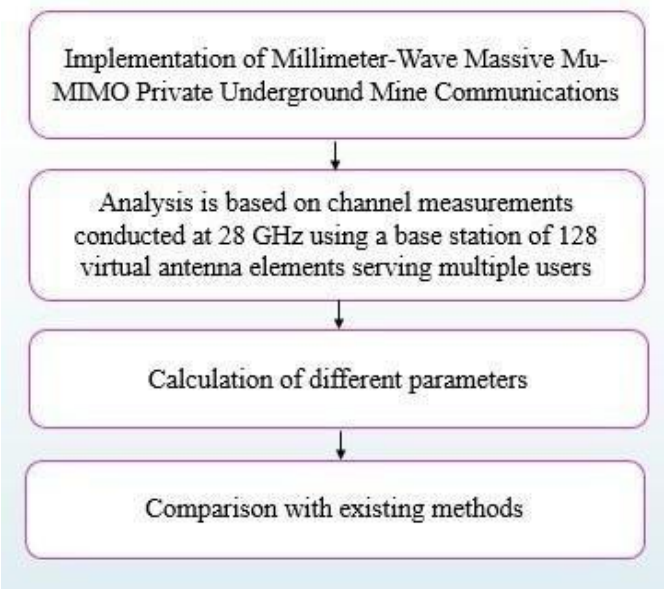

Fig 4: Flow of Proposed Method

4.3 Measurement Procedure

The maximum RF transmit power was fixed at 6 dBm over the 800 MHz bandwidth. The number of sweep points was set to 1201 which corresponds to a maximum excess delay of 1.5μs. Since the VNA takes time to sweep over the measured frequency bands, there were no moving people or objects in the gallery, leading to a static channel. To emulate an uplink massive MU-MIMO system, the Rx subsystem which is considered as a base station (BS), was placed close to the left side wall of the gallery at a height of 1.7 m to form a virtual URA of 64 elements uniformly spaced by $\lambda/2$ and perpendicular to the gallery wall. At the Tx side, the horn antenna was fixed on a tripod with a height of 1.6 m to emulate an active user equipment (UE).

A total of 17 different locations were predefined on the mine galley of which 12 of them are related to LOS links (Tx1–Tx13), and the rest are referred to online of sight (NLOS), as illustrated in Fig.

The Tx horn antenna was aligned (using laser beam tool) to the center of the Rx URA, for all locations, to achieve the maximum received power. For each Tx–Rx combination, the CTF and the CIR were recorded providing a total of 2176 measurements. Finally, Table I summarizes the main parameters regarding the measurement settings. It is worth mentioning that before the measurement campaign, the VNA is first calibrated using Short-Open Load-Thru (SOLT) technique to remove the effect of RF cables and other passive elements in the measurement system.

The CTF H(f) can be derived from the measured transmission parameter S21(f) which can be expressed in the frequency domain as follows

$$S_{21}(f) = H\,(f)\,H_{sys}\,(f)$$

where Hsys(f) is the transfer function of the Tx and Rx link. To measure the impact of the equipment (RFoF link, fiber, and amplifier), reference measurements at 1-m separation distance have been conducted in an anechoic chamber. The measured S21ref(f) parameter can be expressed as follows:

$$S_{21ref}(f) = H_{ref}(f)\,H_{sys}\,(f)$$

Then, the transfer function of the Tx and Rx link equipment can be determined as follows:

$$H_s(f) = \frac{S_{21r}(f)}{H_r(f)}$$

where Href(f) is the free space transfer function.

4.3.1 Path Loss Measurement

Path loss denotes the signal power loss in the propagation channel and is used to determine link budgets by evaluating the propagation loss between the transmitter and the receiver. As a result,

$$\mathrm{PL} = \frac{1}{N_f}\sum_{k=1}^{N_f}|H(f_k)|^2$$

$$H\,(f_k) = \frac{S_{21}(f_k)}{H_{sys}(f_k)}$$

Finally, the wideband path loss can be obtained using the following expression:

$$\mathrm{PL(dB)} = -10\log_{10}\left[\frac{1}{N_f}\sum_{k=1}^{N_f}\left|\frac{S_{21}(f_k)}{H_{sys}(f_k)}\right|^2\right]$$

4.3.2 Path Loss Modeling

Large-scale path loss models are important in designing communication systems . They are used to predict link budgets by estimating the attenuation over the distance of propagating signals. Among different types of large-scale channel models (empirical, stochastic, and deterministic), path loss models based on measurements offer a realistic insight into propagation characteristics .

Thus, two potential path loss models (log-distance and multislope) have been considered in this study. The log-distance path loss model is widely used in wireless communications because it provides a simple and practical way to predict the received signal strength . Hence, the log-distance path loss model can be used to estimate the large-scale fading resulting from multimode propagation in the underground mine . This model is parametrized by PLE parameter n, and it is given by the following equation.

$$\mathrm{PL[dB]} = \mathrm{PL_0[dB]} + 10\ \mathrm{n}\log_{10}\left[\frac{d}{d_0}\right] + \chi_\sigma$$

where PL0 is the path loss at a reference distance d0 (generally taken as 1 m), d is the Tx–Rx separation distance in meters, and $\chi\sigma$ is a zero mean Gaussian random variable with a standard deviation σ in dB.

In fact, the propagation in the mine gallery is based on the hypothesis that propagation takes the form of waveguide transmission .
Therefore, in the LOS scenario, the signal undergoes free space propagation in the near region. Then, a lower attenuation is shown after a particular distance known as the breakpoint distance dbp .

Where PL0 is the path loss at a reference distance d0 (generally taken as 1 m), d is the Tx–Rx separation distance in meters, and $\chi\sigma$ is a zero mean Gaussian random variable with a standard deviation σ in dB.

In fact, the propagation in the mine gallery is based on the hypothesis that propagation takes the form of waveguide transmission.

Therefore, in the LOS scenario, the signal undergoes free space propagation in the near region. Then, a lower attenuation is shown after a particular distance known as the breakpoint distance dbp .

At the end of the LOS segment, the signal encounters a higher attenuation in the NLOS segment between 60 and 80 m. As a result, a multislope path loss model is proposed for a better modeling of the wave propagation in the underground mining gallery. In a typical indoor and outdoor environment, separate path loss models are used for LOS and NLOS scenarios. However, in tunnel propagation, a more effective approach is to combine these path loss models into a single multislope path loss model and The multislope path loss model is given by PL[dB] .

$$= \begin{cases} \mathrm{PL}_0 + 10n_1\log_{10}\left(\dfrac{d}{d_0}\right) + \chi_{\sigma_1}, & \text{for } d \le d_{\mathrm{bp}} \\ \mathrm{PL}_{\mathrm{bp}} + 10n_2\log_{10}\left(\dfrac{d}{d_{\mathrm{bp}}}\right) + \chi_{\sigma_2}, & \text{for } d_{\mathrm{bp}} \le d \le d_{\mathrm{LOS}} \\ \mathrm{PL}_{\mathrm{LOS}} + 10n_3\log_{10}\left(\dfrac{d}{d_{\mathrm{LOS}}}\right) + \chi_{\sigma_3}, & \text{for } d \ge d_{\mathrm{LOS}} \end{cases}$$

where PLbp is the path loss at the breakpoint distance dbp, PLLOS is the path loss at the maximum LOS distance (dLOS = 60 m), n1, n2 and n3 are the PLEs, χσ1 , χσ2 ,3 χσ and zero mean Gaussian variables with standard deviation of σ1, σ2, and σ3, respectively.

CHAPTER 5

ADVANTAGES AND APPLICATIONS

5.1 Advantages

128 BS antennas has low BER at desired level.

128 BS antennas has high throughput and capacity which is more than existing method.

5.2 Applications

Applications of are:

MIMO environments,

Beam Forming,

Satellite Communication.

CHAPTER 6
SOFTWARE & HARDWARE REQUIREMENTS

6.1 Software Requirements

Matlab 2022b or above

6.2 Hardware Requirements

Operating Systems:

Windows 10

Windows 7 Service Pack 1

Windows Server 2019

Windows Server 2016 Processors:
Minimum: Any Intel or AMD x86-64 processor
Recommended: Any Intel or AMD x86-64 processor with four logical cores and AVX2 instruction set support Disk:
Minimum: 2.9 GB of HDD space for MATLAB only, 5-8 GB for a typical installation
Recommended: An SSD is recommended A full installation of all MathWorks products may take up to 29 GB of disk space
RAM: Minimum: 4 GB Recommended: 8 GB

CHAPTER 7

MATLAB

7.1 Introduction To MATLAB

The name MATLAB stands for Matrix Laboratory. The software is built up around vectors and matrices. This makes the software particularly useful for linear algebra but MATLAB is also a great tool for solving algebraic and differential equations and for numerical integration. MATLAB has powerful graphic tools and can produce nice pictures in both 2D and 3D. It is also a programming language, and is one of the easiest programming languages for writing mathematical programs. These factors make MATLAB an excellent tool for teaching and research.

MATLAB was written originally to provide easy access to matrix software developed by the LINPACK (linear system package) and EISPACK (Eigen system package) projects. It integrates computation, visualization, and programming environment. Furthermore, MATLAB is a modern programming language environment: it has sophisticated data structures, contains built-in editing and debugging tools, and supports object-oriented programming. MATLAB has many advantages compared to conventional computer languages (e.g., C, FORTRAN) for solving technical problems.

MATLAB abilities a family of add-on software program utility software application software program software utility software-unique solutions called toolboxes. Very essential to maximum customers of MATLAB, toolboxes assist you to studies and observe specialized technology. Toolboxes are entire collections of MATLAB abilities (M-files) that increase the MATLAB surroundings to remedy precise schooling of problems. Areas in which toolboxes are to be had embody signal processing, manipulate systems, neural networks, fuzzy correct judgment,wavelets, simulation, and hundreds of others.

MATLAB abilities a family of add-on software program utility software application software program software utility software-unique solutions called toolboxes. Very essential to maximum customers of MATLAB, toolboxes assist you to studies and observe specialized technology. Toolboxes are entire collections of MATLAB abilities (M-files) that increase the MATLAB surroundings to remedy precise schooling of problems. Areas in which toolboxes are to be had embody signal processing, manipulate systems, neural .

7.2 Brief History of MATLAB

It has powerful built-in routines that enable a very wide variety of computations. It also has easy to use graphics commands that make the visualization of results immediately available.

Specific applications are collected in packages referred to as toolbox. There are toolboxes for signal processing, symbolic computation, control theory, simulation, optimization, and several other fields of applied science and engineering. MATLAB is an interactive system whose basic data element is an array that does not require dimensioning. The software package has been commercially available since 1984 and is now considered as a standard tool at most universities and industries worldwide.

Cleve Moler, the chairman of the computer science department at the University of New Mexico, started developing MATLAB in the late 1970s. The first MATLAB® was not a programming language; it was a simple interactive matrix calculator. There were no programs, no toolboxes, no graphics and no ODEs or FFTs. He designed it to give his student's access to LINPACK and EISPACK without them having to learn FORTRAN. It soon spread to other universities and found a strong audience within the applied mathematics community. The mathematical basis for the first version of MATLAB was a series of research papers by J. H. Wilkinson and 18 of his colleagues, published between 1965 and 1970 and later collected in Handbook for Automatic Computation, Volume II, Linear Algebra, edited by Wilkinson and C. Reinsch. These papers present algorithms, implemented in Algol 60, for solving matrix linear equation and Eigen value problems.

Cleve Moler, the chairman of the computer science department at the University of New Mexico, started developing MATLAB in the late 1970s. The first MATLAB® was not a programming language; it was a simple interactive matrix calculator. There were no programs, no toolboxes, no graphics and no ODEs or FFTs. He designed it to give his student's access to LINPACK and EISPACK without them having to learn FORTRAN. It soon spread to other universities and found a strong audience within the applied mathematics community. The mathematical basis for the first version of MATLAB was a series of research papers by J. H. Wilkinson and 18 of his colleagues, published between 1965 and 1970 and later collected in Handbook for Automatic Computation, Volume II, Linear Algebra, edited by Wilkinson and C. Reinsch. These papers present algorithms, implemented in Algol 60, for solving matrix linear equation and Eigen value problems.

In the 1970s and early 1980s, I was teaching Linear Algebra and Numerical Analysis at the University of New Mexico and wanted my students to have easy access to LINPACK and EISPACK without writing FORTRAN programs. By "easy access," I meant not going through the remote batch processing and the repeated editcompile-link- load-execute process that was ordinarily required on the campus central mainframe computer. Jack little, an engineer, was exposed to it during a visit Moler made to Stanford University in 1983. Recognizing its commercial potential, he joined with Moler and Steve Bangert. They rewrote MATLAB in C and founded Math Works in 1984 to continue its development. These rewritten libraries were known as JACKPAC. In 2000, MATLAB was rewritten to use a newer set of libraries for matrix

manipulation, LAPACK. MATLAB was first adopted by researchers and practitioners in control engineering, little's specialty, but quickly spread to many other domains. It is now also used in education, in particular the teaching of linear algebra and numerical analysis, and is popular amongst scientists involved in video processing.

7.3 EISPACK and LINPACK

In 1970, a group of researchers at Argonne National Laboratory proposed to the U.S. National Science Foundation (NSF) to "explore the methodology, costs, and resources required to produce, test, and disseminate high-quality mathematical software and to test, certify, disseminate, and support packages of mathematical software in certain problem areas." The group developed EISPACK (Matrix Eigen system Package) by translating the Algol procedures for Eigen value problems in the handbook into FORTRAN and working extensively on testing and portability. The first version of EISPACK was released in 1971 and the second in 1976.

In 1975, four of us Jack Dongarra, Pete Stewart, Jim Bunch, and myself proposed to the NSF another research project that would investigate methods for the development of mathematical software. A byproduct would be the software itself, dubbed LINPACK, for Linear Equation Package. This project was also centered at Argonne. LINPACK originated in FORTRAN; it did not involve translation from Algol. The package contained 44 subroutines in each of four numeric precisions. In a sense, the LINPACK and EISPACK projects were failures. We had proposed research projects to the NSF to "explore the methodology, costs, and resources required to produce, test, and disseminate high-quality mathematical software." We never wrote a report or paper addressing those objectives. We only produced software.

So, I studied Niklaus Wirth's book Algorithms + Data Structures = Programs and learned how to parse programming languages. I wrote the first MATLAB an acronym for Matrix Laboratory in FORTRAN, with matrix as the only data type. The project was a kind of hobby, a new aspect of programming for me to learn and something for my students to use. There was never any formal outside support, and certainly no business plan. This first MATLAB was just an interactive matrix calculator. This snapshot of the start-up screen shows all the reserved words and functions. There are only 71. To add another function, you had to get the source code from me, write a FORTRAN subroutine, add your function name to the parse table, and recompile MATLAB.

7.4 Starting MATLAB

After logging into your account, you can enter
MATLAB by double-clicking on the MATLAB shortcut icon (MATLAB 7.0.4) on your Windows desktop.

window called the MATLAB desktop appears.

- The Command Window
- The Command History
- The Workspace The
- Current Directory The
- Help Browser

7.4.1 Current Folder

This panel allows you to access the project folders and files.

Command Window: This is the main area where commands can be entered at the command line. It is indicated by the command prompt (>>).

7.4.2 Workspace

The workspace shows all the variables created and/or imported from files.

7.4.3 Command History

This panel shows or return commands that are entered at the command line.

7.4.4 Help Browser

The critical way to get assist online is to use the MATLAB help browser, opened as a separate window every through clicking at the question mark photograph (?) on the computing tool toolbar, or through manner of typing assist browser on the spark off in the command window. The assist Browser is an internet browser blanketed into the MATLAB computing tool that shows a Hypertext Markup Language (HTML) files. The Help Browser consists of panes, the help navigator pane, used to find out information, and the show pane, used to view the information. Self- explanatory tabs apart from navigator pane are used to performs are searching out.

7.5 MATLAB language

This is a high-level matrix/array language with control flow statements, functions, data stru ctures, input/output, and object-oriented programming features. It allows both "programming in the small" to rapidly create quick and dirty throw-away programs, and

7.6 **MATLAB working environment**

This is the set of tools and facilities that you work with as the MATLAB user or programmer. It includes facilities for managing the variables in your workspace and importing and exporting data. It also includes tools for developing, managing, debugging, and profiling M-files, MATLAB's applications.

7.7 MATLAB mathematical function library

This is a vast collection of computational algorithms ranging from elementary functions like sum, sine, cosine, and complex arithmetic, to more sophisticated functions like matrix inverse, matrix eigenvalues, Bessel functions, and fast Fourier transforms.

7.8 MATLAB Application Program Interface (API)

This is a library that allows you to write C and FORTRAN programs that interact with MATLAB. It includes facilities for calling routines from MATLAB (dynamic linking), calling MATLAB as acomputational engine, and for reading and writing MAT-files.

7.9 MATLAB DESKTOP

MATLAB Desktop is the precept MATLAB utility window. The computing tool includes five sub home windows, the command window, the workspace browser, the modern-dayday list window, the command records window, and one or greater decide domestic windows, which is probably confirmed high-quality on the identical time due to the truth the client suggests a photo. The command window is in which the character types MATLAB instructions and expressions at the spark off (>>) and in which the output of these commands is displayed. MATLAB defines the workspace because the set of variables that the client creates in a bit consultation. The workspace browser suggests those variables and some facts about them. Double clicking on a variable within the workspace browser launches the Array Editor, which may be used to gain statistics and profits instances edit exceptional homes of the variable.

The modern-day-day-day Directory tab above the workspace tab suggests the contents of the cutting-edge list, whose path is shown inside the modern-day list window. For example, in the home windows on foot machine the path is probably as follows: C:

Clicking at the button to the right of the window permits the individual to trade the present day listing. MATLAB uses a seeking out path to find out M- documents and one-of-a-type MATLAB associated documents, which can be put together in directories within the computer document tool. Any report run in MATLAB need to be dwelling in the modernday-day listing or in a list that is on is looking for course. By default, the documents supplied with MATLAB and math works toolboxes are included inside the searching out direction. The first-rate manner to look which directories are on the searching out route. The satisfactory manner to appearance which directories are speedy the quest route, or to characteristic or regulate a searching for course, is to pick out outset path from the File menu the computing device, and then use the set course talk discipline. It is proper exercise to feature any generally used directories to the hunt route to avoid again and again having the exchange the cutting-edge-day listing.

The Command History Window contains a file of the instructions a person has entered in the command window, together with every contemporary-day and former MATLAB periods. Previously entered MATLAB instructions can be determined on and re-completed from the command statistics window thru proper clicking on a command or series of commands. This movement launches a menu from which to select numerous options similarly to executing the commands. This is useful to select out abilities options in addition to executing the instructions. This is a beneficial feature at the equal time as experimenting with numerous commands in a piece session.

7.10 Using the MATLAB Editor to create M-Files

The MATLAB editorial manager is a literary substance proofreader particular for growing M-facts and a graphical MATLAB debugger. The supervisor can seem in a window through command facts technique for itself, or it is probably a right-clicking inside the PC. M-information this gadget signified through the use of the expansion .M, as in pixel up.M. The MATLAB editorial supervisor window has a few draws down menus for obligations collectively with sparing, seeing, and troubleshooting facts. Since it plays more than one easy test and furthermore affects utilization of shade to separate among exclusive variables of code, this article editorial supervisor is often supported due to reality the system of a need for composing and altering M-talents. To open the manager, type at enact opens the Mdocument filename. M in a supervisor window, sorted out for enhancing.

7.11 Features of MATLAB

It also provides an interactive environment for iterative exploration, design and problem solving.

It provides vast library of mathematical functions for linear algebra, statistics, Fourier analysis, filtering, optimization, numerical integration and solving ordinary differential equations.

It provides built-in graphics for visualizing data and tools for creating custom plots.

MATLAB's programming interface gives development tools for maintainability and maximizing performance.

It provides tools for building applications with custom graphical interfaces.

It provides functions for integrating MATLAB based algorithms with external applications and languages such as C, Java, .NET and

Microsoft Excel.

7.12 Uses of MATLAB

MATLAB is widely used as a computational tool in science and engineering encompassing the fields of physics, chemistry, math and all engineering streams. It is used in a range of applications including

- Signal Processing and Communications
- Video and Video Processing
- Control Systems
- Test and Measurement
- Computational Finance
- Computational Biology

7.13 Applications of MATLAB

- Statistics and machine learning (ML),This toolbox in MATLAB can be very handy for the programmers. Statistical methods such as descriptive or inferential can be easily implemented. So is the case with machine learning.

- Curve fitting, the curve fitting toolbox helps to analyze the pattern of occurrence of data. After a particular trend which can be a curve or surface is obtained, its future trends can be predicted. Further plotting, calculating integrals, derivatives, interpolation, etc. can be done.
- Control systems Systems nature can be obtained. Factors such as closed-loop, open- loop, its controllability and observability, Bode plot, NY Quist plot, etc. can be obtained. Various controlling techniques such as PD, PI and PID can be visualized. Analysis can be done in the time domain or frequency domain.

- Signal processing, Signals and systems and digital signal processing are taught in various engineering streams. But MATLAB provides the opportunity for proper visualization of this. Various transforms such as Laplace, Z, etc. can be done on any given signal. Theorems can be validated. Analysis can be done in the time domain or frequency domain. There are multiple built-in functions that can be used.

- Mapping, Mapping has multiple applications in various domains. For example, in Big Data, the Map Reduce tool is quite important which has multiple applications in the real world. Theft analysis or financial fraud detection, regression models, contingency analysis, predicting techniques in social media, data monitoring, etc. can be done by data mapping.

- Deep learning, It's a subclass of machine learning which can be used for speech recognition, financial fraud detection, and medical video analysis. Tools such as timeseries, Artificial neural network (ANN), Fuzzy logic or combination of such tools can be employed.
- Financial analysis, An entrepreneur before starting any endeavor needs to do a proper survey and the financial analysis in order to plan the course of action. The tools needed for this are all available in MATLAB. Elements such as profitability, solvency, liquidity, and stability can be identified. Business valuation, capital budgeting, cost of capital, etc. can be evaluated.
- Video processing, The most common application that we observe almost every day are bar code scanners, selfie (face beauty, blurring the background, face detection), video enhancement, etc. The digital video processing also plays quite an important role in transmitting data from far off satellites and receiving and decoding it in the same way. Algorithms to support all such applications are available.

Text analysis, Based on the text, sentiment analysis can be done. Google gives millions of search results for any text entered within a few milliseconds. All this is possible because of text analysis. Handwriting comparison in forensics can be done. No limit to the application and just one software which can do this all.

- Electrical vehicle designing, Used for modeling electric vehicles and analyze their performance with a change in system inputs. Speed torque comparison, designing and simulating of a vehicle, whatnot.
- Aerospace, This toolbox in MATLAB is used for analyzing the navigation and to visualize flight simulator.
- Audio toolbox
- Provides tools for audio processing, speech analysis, and acoustic measurement. It also provides algorithms for audio and speech feature extraction and audio signal transformation.

7.14 Communication

Communications System Toolbox™ offers algorithms and gear for the layout, simulation, and analysis of communications systems. These capabilities are furnished as MATLAB ® features, MATLAB System gadgets™, and Simulink ® blocks. The machine toolbox includes algorithms for source coding, channel coding, interleaving,modulation, equalization, synchronization, and channel modeling. Tools are supplied for bit blunders charge evaluation, producing eye and constellation diagrams, and visualizing channel characteristics. The machine toolbox additionally provides adaptive algorithms that allow

7.15 Key Features

Algorithms for designing the physical layer of communications systems, which includes supply coding, channel coding, interleaving, modulation, channel fashions, MIMO, equalization, and synchronization, GPU-enabled System objects for computationally intensive, algorithms together with Turbo, LDPC, and Viterbi decoders

Interactive visualization equipment,consisting of eye diagrams, constellations, and channel scattering capabilities

Graphical tool for evaluating the simulated bit mistakes rate of a machine with analytical outcomes

Channel models, consisting of AWGN, Multipath Rayleigh Fading, Rician Fading,

MIMO Multipath Fading, and LTE MIMO

7.16 Multipath Fading

Basic RF impairments, along with nonlinearity, section noise, thermal noise, and section and frequency offsets

Algorithms available as MATLAB features, MATLAB System objects, and Simulink blocks

Support for fixed-point modeling and C and HDL code technology System Design,

Charecterization and visualizatio

The layout and simulation of a communications gadget requires analyzing its reaction to the noise and interference inherent in real-world environments, reading its behavior the usage of graphical and quantitative manner, and determining whether the resulting overall performance meets requirements of acceptability. Communications System Toolbox implements a selection of obligations for communications machine layout and simulation. Many of the functions, System objects™, and blocks inside the device toolbox perform computations associated with a specific thing of a communications gadget, consisting of a demodulator or equalizer. Other talents are designed for visualization or evaluation.

7.17 System Characterization

The system toolbox offers several standard methods for quantitatively characterizing system performance:

BER simulations: BER tool— A graphical user interface that enables you to analyze BER performance of communications systems. You can analyze performance via a simulationbased, semi analytic, or theoretical approach.

Error Rate Test Console — A MATLAB object that runs simulations for communications systems to measure error rate performance. It supports user-specified test points and

generation of parametric performance plots and surfaces. Accelerated performance can be realized when running on a multi core computing platform.

Multi core and GPU acceleration — A capability provided by Parallel Computing Toolbox™ that enables you to accelerate simulation performance using multi core and GPU hardware within your computer.

Distributed computing and cloud computing support — Capabilities provided by Parallel Computing Toolbox and MATLAB Distributed Computing Server™ that enable you to leverage the computing power of your server farms and the Amazon EC2 Web service. Performance Visualization. The system toolbox provides the following capabilities for visualizing system performance: Channel visualization tool — For visualizing the characteristics of a fading channel.

Eye diagrams and signal constellation scatter plots — for a qualitative, visul understanding of system behavior that enables you to make initial design decisions

Signal trajectory plots — for a continuous picture of the signal's trajectory between decision points

BER plots — for visualizing quantitative BER performance of a design candidate, parameterized by metrics such as SNR and fixed-point word size

7.18 Analog and Digital Modulation

Analog and digital modulation strategies encode the facts circulation into a sign this is appropriate for transmission. Communications System Toolbox presents some of modulation and corresponding demodulation abilities. These talents are available as MATLAB features and gadgets, MATLAB System Modulation sorts provided by the toolbox are:

Source and Channel Coding

Communications System Toolbox affords source and channel coding talents that can help you develop and compare communications architectures fast, enabling you to discover what-if eventualities and avoid the need to create coding competencies from scratch.

Source Coding

Source coding, also referred to as quantization or signal formatting, is a manner of processing facts a good way to lessen redundancy or prepare it for later processing. The system toolbox offers a diffusion of styles of algorithms for imposing source coding and interpreting, inclusive of:

- Quantizing
- Companding (μ-law and A-law)
- Differential pulse code modulation (DPCM)
- Huffman coding
- Arithmetic coding
- orthogonal area-time block code (OSTBC) (encoder and decoder for MIMO channels)
- Turbo encoder and decoder examples The gadget toolbox offers application functions for developing your personal channel coding.
- You can create generator polynomials and coefficients and syndrome deciphering tables, in addition to product parity-take a look at and generator matrices.

Convolutional, including General multiplexed interleaver, convolutional interleaver, and helical

7.19 Channel Modeling and RF Impairments

Communications System Toolbox provides algorithms and tools for modeling noise, fading, interference, and different distortions which might be commonly found in communications channels. The system toolbox supports the subsequent styles of channels:

Additive white Gaussian noise (AWGN)
Multiple-enter multiple-output (MIMO) fading
Single-enter single-output (SISO), Rayleigh, and Rician fading
Binary symmetric
A MATLAB channel object provides a concise, configurable implementation of channel models, enabling you to specify parameters such as:

- Path delays
- Average path gains
- Maximum Doppler shifts
- K-Factor for Rician fading channels
- Doppler spectrum parameters

RF Impairments To model the effects of a non-ideal RF front end, you can introduce the following impairments into your communications system, enabling you to explore and characterize performance with real-world effects:

Memory less nonlinearity
Phase and frequency offset
Phase noise
Thermal noise You can include more complex RF impairments and RF circuit models in your design using SimRF™.

7.20 Equalization and Synchronization

Communications System Toolbox lets you discover equalization and Synchronization strategies.

These techniques are usually adaptive in nature and tough to design and symbolize. The machine

LMS

Normalized LMS

Variable step LMS

Signed LMS

MLSE (Viterbi)

RLS

CMA

These adaptive equalizers are available as nonlinear decision feedback equalizer (DFE) implementations and as Linear (symbol or fractionally spaced) equalizer implementations. Synchronization The device toolbox provides algorithms for each service segment synchronization and timing phase synchronization. For timing section synchronization, the machine toolbox presents a MATLAB Timing Phase Synchronizer object that offers the following implementation techniques:

Early-late gate timing method Gardner's

Fourth-order nonlinearity method

Stream Processing in MATLAB and Simulink Most verbal exchange structures cope with streaming and frame-primarily based statistics using a aggregate of temporal processing and simultaneous multi frequency and multichannel processing. This form of streaming multidimensional processing can be visible in superior communication architectures consisting of OFDM and MIMO. Communications System Toolbox enables the simulation of advanced communications structures via helping move processing and frame-based simulation in MATLAB and Simulink. In MATLAB, circulate processing is enabled by way of System items™, which use MATLAB objects to symbolize time-based and facts-driven algorithms, sources, and sinks. System objects implicitly manipulate many information of flow processing, including information indexing, buffering, and management of set of rules state. You can mix System gadgets with fashionable MATLAB functions and operators. Most System items have a corresponding Simulink block with the identical abilities. Simulink handles circulation processing implicitly with the aid of coping with the float of information thru the blocks that make up a Simulink model. Simulink is an interactive graphical environment for modeling and simulating dynamic systems that uses hierarchical diagrams to

symbolize a machine version. It includes a library of widespread- reason, predefined blocks to represent algorithms, resources, sinks, and device hierarchy.

Implementing a Communications System Fixed-Point Modeling Many communications systems use hardware that requires a fixed-point representation of your design.
Communications System Toolbox supports fixed-point modeling in all relevant blocks and System objects™ with tools that help you configure fixed-point attributes.

7.21 Fixed-point support in the system toolbox includes

Word sizes from 1 to 128 bits

Arbitrary binary-point placement

Overflow handling methods (wrap or saturation)

Rounding methods: ceiling, convergent, floor, nearest, round, simplest, and zero FixedPoint Tool in Simulink Fixed Point™ facilitates the conversion of floating-point data types to fixed point. For configuration of fixed-point
properties, the tool tracks overflows and maxima and minima.

7.22 Code Generation

Once you've got advanced your set of rules or communications device, you can robotically generate C code from it for verification, rapid prototyping, and implementation. Most System gadgets, functions, and blocks in Communications System Toolbox can generate ANSI/ISO C code the use of MATLAB Coder™, Simulink Coder™, or Embedded Coder™. A subset of System gadgets and Simulink blocks also can generate HDL code. To leverage present highbrow belongings, you can choose optimizations for specific processor architectures and integrate legacy C code with the generated code. You can also generate C code for both floating- point and fixed-point data types. DSP Proto typing DSPs are used in communication system implementation for verification, rapid prototyping, or final hardware implementation. Using the processor-in-the-loop (PIL) simulation capability found in Embedded Coder, you can verify generated source code and compiled code by running your algorithm’s implementation code on a target processor. FPGA Prototyping FPGAs are used in communication systems for implementing high-speed signal processing algorithms. Using the FPGA-in-the-loop (FIL) capability found in HDL Verifier™, you can test RTL code in real hardware for any existing HDL code, either manually written or automatically generated HDL code.

7.23 Learning outcomes

Introduction to Matlab

What is EISPACK & LINPACK

How to start with MATLAB About Matlab

language Matlab coding skills About tools

& libraries

Application Program Interface in Matlab
About Matlab desktop

How to use Matlab editor to create M-Files Features of Matlab

Basics on Matlab

What is an Image/pixel? About image formats

Introduction to Image Processing How digital image is formed

Importing the image via image acquisition tools Analyzing and manipulation of

image.

Acquisition

Image enhancement

Image restoration
Color image processing

Segmentation etc.,

How to extend our work to another real time applications Project development

Skills

Problem analyzing skills
Problem solving skills
Creativity and imaginary skills
Programming skills
Deployment
Testing skills
Debugging skills
Project presentation skills
Thesis writing skills

CHAPTER 8

RESULTS

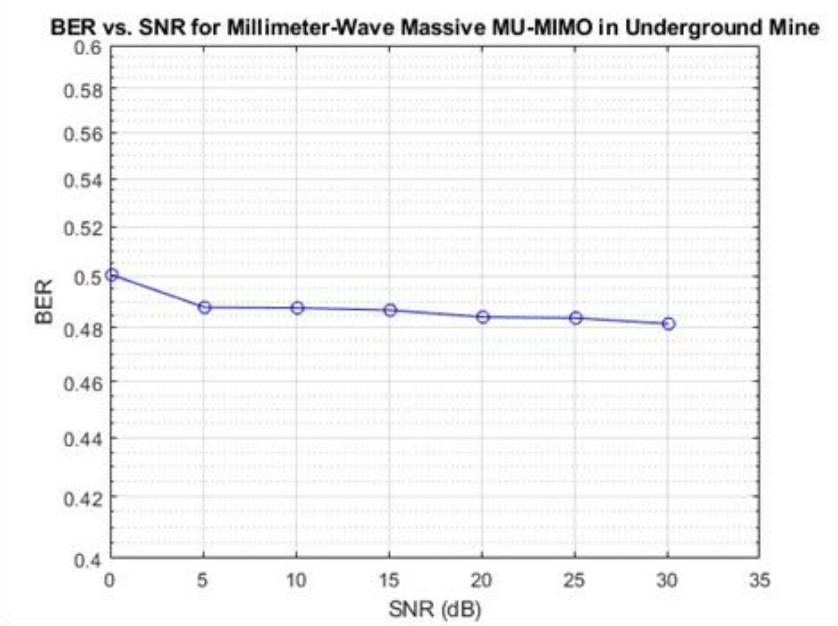

Fig 5: Bit Error Rate VS Signal to Noise Ratio

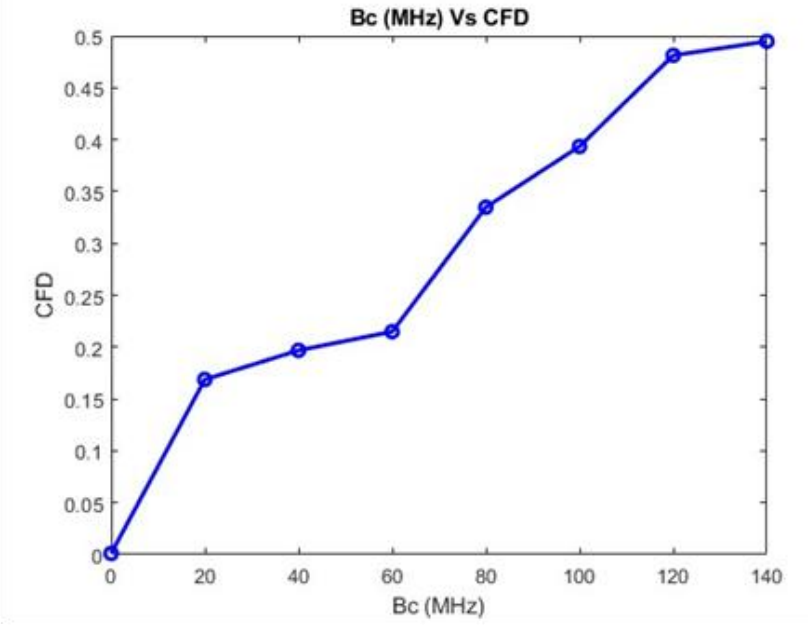

Fig 6: Cumulative Frequency Distribution VS Coherence Bandwidth

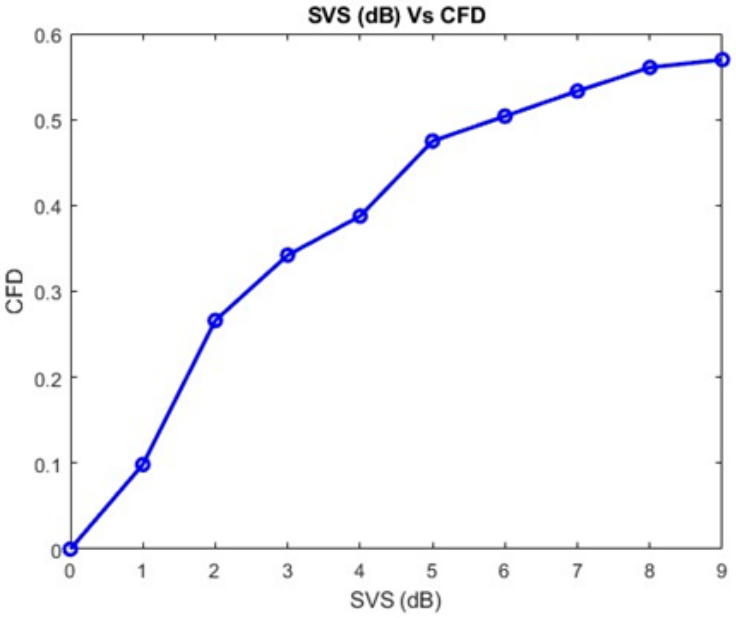

Fig 7: Cumulative Frequency Distribution VS Singular Value Spread

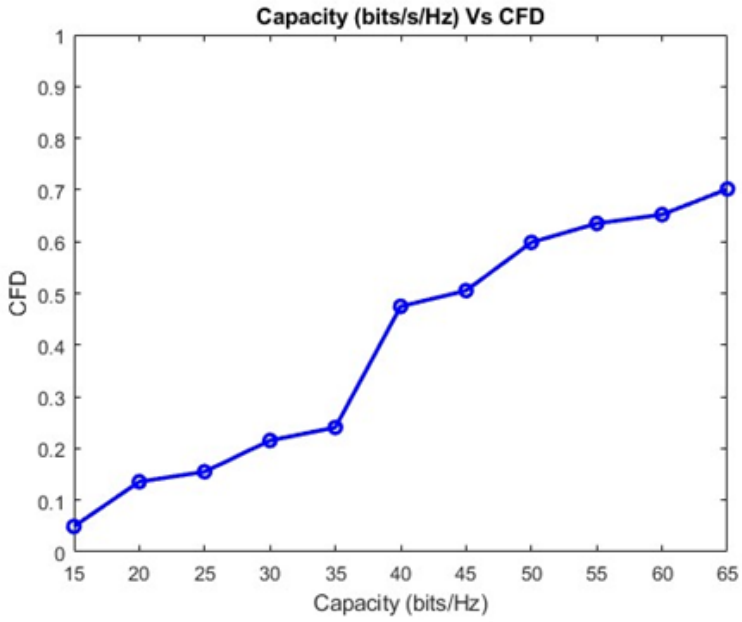

Fig 8: Cumulative Frequency Distribution VS Capacity

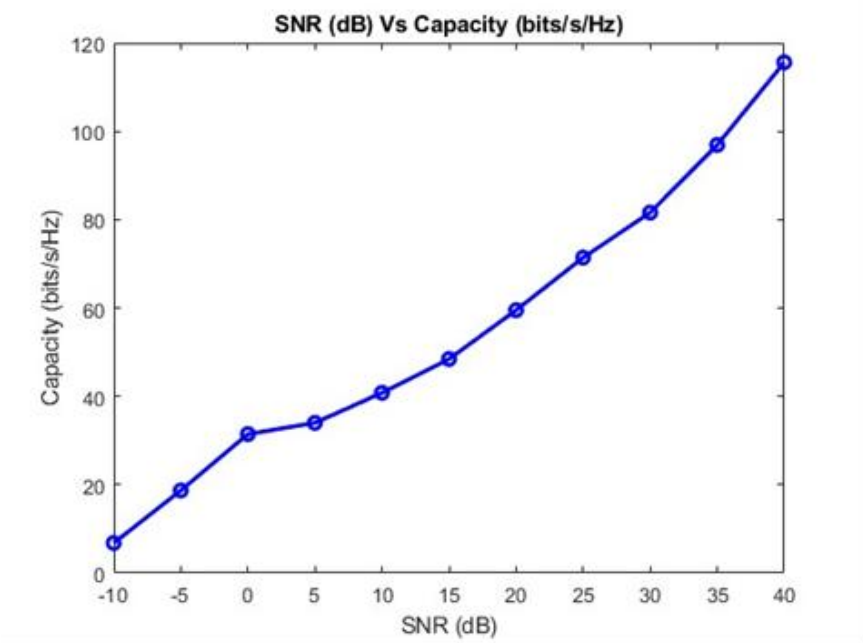

Fig 9: Capacity VS Signal to Noise Ratio

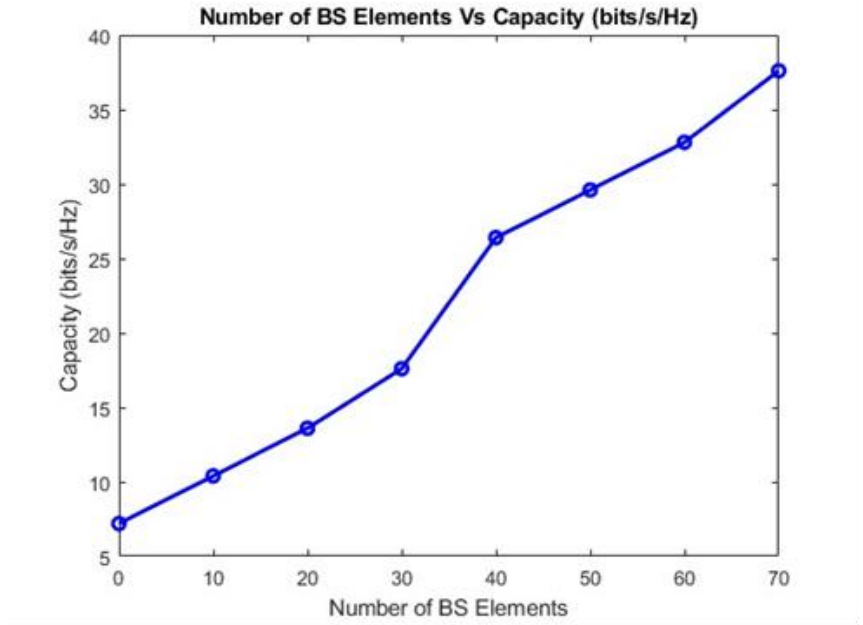

Fig 10:Capacity VS Number of BS Elements

CHAPTER 9
CONCLUSION & FUTURE SCOPE

CONCLUSION

After the implementation of 128 antenna at the Base Station in contrast to 64 BS antennas in existing method, we can finally conclude that, the proposed implementation with 128 BS antennas has performed well, not only it produced better BER and capacity than the existing implementation but, it stood at even low SNR environments unlike existing method.

FUTURE SCOPE

- AI-Driven Beamforming – Implementing machine learning algorithms to
- optimize beamforming and resource allocation dynamically.
- 5G and 6G Integration – Extending the research to future wireless technologies
- for enhanced underground mine communications.
- Energy-Efficient MIMO Systems – Developing low-power massive MIMO
- architectures to reduce energy consumption while maintaining performance.
- Advanced Channel Modeling – Refining path loss and multipath propagation
- models to better predict real-time signal behavior in underground environments.
- IoT and Industrial Automation – Leveraging MIMO technology for real-time
- monitoring and automation in smart mining operations.

REFERENCES

1. J. Lööw, L. Abrahamsson, and J. Johansson, "Mining 4.0—The impact of new technology from a work place perspective," Mining, Metall. Exploration, vol. 36, no. 4, pp. 701–707, Aug. 2019, doi: 10.1007/s42461-019-00104-9.
2. S. M. Riurean, M. Leba, and A. C. Ionica, "Conventional and advanced technologies for wireless transmission in underground mine," in Application of Visible Light Wireless Communication in Underground Mine. Cham, Switzerland: Springer, 2021, pp. 41–125.
3. M. Ghaddar, I. Ben Mabrouk, M. Nedil, K. Hettak, and L. Talbi, "Deterministic modeling of 5G millimeter-wave communication in an underground mine tunnel," IEEE Access, vol. 7, pp. 116519–116528, 2019.
4. O. Kolade and L. Cheng, "Markov model characterization of a multicarrier narrowband powerline channel with memory in an underground mining environment," IEEE Access, vol. 9, pp. 59085–59092, 2021.
5. R. Flamini et al., "Toward a heterogeneous smart electromagnetic environment for millimeter-wave communications: An industrial view-point," IEEE Trans. Antennas Propag., vol. 70, no. 10, pp. 8898–8910, Oct. 2022.
6. T. S. Rappaport, G. R. MacCartney, M. K. Samimi, and S. Sun, "Wideband millimeter- wave propagation measurements and channel models for future wireless communication system design," IEEE Trans. Commun., vol. 63, no. 9,
pp. 3029–3056, Sep. 2015.
7. G. R. Maccartney, T. S. Rappaport, S. Sun, and S. Deng, "Indoor office wideband millimeter-wave propagation measurements and channel models at 28 and 73 GHz for ultradense 5G wireless networks," IEEE Access, vol. 3, pp. 2388– 2424, 2015.
8 .J.-Y. Lee, J.-H. Lee, and S.-C. Kim, "Improving the accuracy of millimeter-wave ray-tracin simulations by modeling roadside trees," IEEE Antennas Wireless Propag.
Lett., vol. 18, no. 1, pp. 162–166, Jan. 2019.
9. X. Gao, O. Edfors, F. Rusek, and F. Tufvesson, "Massive MIMO performance evaluation based on measured propagation data," IEEE Trans. Wireless Commun., vol.
14, no. 7, pp. 3899– 3911, Jul. 2015.
10. S. Mumtaz, J. Rodriguez, and L. Dai, "mmWave Massive MIMO: A Paradigm for5G. New York, NY, USA: Academic, 2016.

11. J. Huang, C.-X. Wang, R. Feng, J. Sun, W. Zhang, and Y. Yang, "Multi- frequency mmWave massive MIMO channel measurements and characterization for 5G wireless communication systems," IEEE J. Sel. Areas Commun., vol. 35, no. 7, pp. 1591–1605, Jul. 2017.
12. M. Shafi et al., "5G: A tutorial overview of standards, trials, challenges, deployment, and practice," IEEE J. Sel. Areas Commun., vol. 35, no. 6, pp. 1201–1221, Jun. 2017.
13. S. A. M. Tariq, C. L. Despins, S. Affes, and C. Nerguizian, "Angular dispersion of a scattered underground wireless channel at 60 GHz," IEEE Access, vol. 8, pp. 67572– 67580, 2020.
14. M. Jadoul. (2021). Here is Why Mining is Digging Into 5G. [Blog] NOKIA. [Online]. Available: https://www.nokia.com/blog/here-is-whymining-is- digging-into-5g/ .
15. C. Wang, W. Ji, G. Zheng, and A. Saleem, "Analysis of propagation characteristics for various subway tunnel scenarios at 28 GHz," Int. J. Antennas Propag., vol. 2021, pp. 1– 16, Sep. 2021.

ANNEXURE – A

SOURCE CODE

```
clear close all
clc

%%
% Implementation
%Simulations
BWE = 800e6; %800 MHz txantGE = 20;
%20dBi rxantGE = 1; %1Bi PtxE = 6;
%6dBm swpptsE = 1201;  %sweep points
txheitE = 1.6;   %Transmitter Height
rxheitE = 1.7;   %Receiver Height

% Simulation parameters numUsersE = 10; % Number of users
numBSantennasE = 128; % Number of base station antennas
numSubcarriersE = 1024; % Number of subcarriers snrRangeE =
0.1:5:35; % SNR range in dB
numMonteCarloE = 10; % Number of Monte Carlo simulations

% Path loss model parameters (example values for underground mine)
frequencyE = 28e9; % 28 GHz distanceE = 100; % Distance in meters
pathLossExponentE = 2.2; % Path loss exponent for underground environment
shadowingStdDevE = 6; % Shadowing standard deviation in dB

% Pre-allocate channel matrix
HE = zeros(numBSantennasE, numUsersE, numSubcarriersE);

% Pre-allocate for BER results
BERE = zeros(length(snrRangeE), numUsersE);

for mcE = 1:numMonteCarloE     for subcE = 1:numSubcarriersE         for
uE = 1:numUsersE            pathLossE = 10^(-pathLossExponentE *
log10(distanceE));            shadowingE = 10^(shadowingStdDevE * randn
/ 10);
          HE(:,uE,subcE) = (pathLossE * shadowingE) * (randn(numBSantennasE, 1) +
1j*randn(numBSantennasE, 1)) / sqrt(2);         end
   end



  % Noise power
 noisePowerE = 10.^(-snrRangeE/10);

 for snrIdxE = 1:length(snrRangeE)
  snrE = snrRangeE(snrIdxE);
```

```
% Transmit signal
bitsPerSymbolE = 4; % for 16-QAM
txSignalE = randi([0 1], numUsersE, numSubcarriersE * bitsPerSymbolE);

txModSignalE = zeros(numUsersE, numSubcarriersE);
for uE = 1:numUsersE % Reshape bits to symbols
  reshapedBitsE = reshape(txSignalE(uE,:), [], bitsPerSymbolE);
  txModSignalE(uE,:) = reshape(qammod(reshapedBitsE, 16, 'InputType', 'bit',
'UnitAveragePower', true),[],1);
end

% MU-MIMO processing (ZF precoding)
WE = zeros(numBSantennasE, numUsersE, numSubcarriersE); for
subcE = 1:numSubcarriersE
  WE(:,:,subcE) = (HE(:,:,subcE)' / (HE(:,:,subcE) * HE(:,:,subcE)' +
eye(numBSantennasE)/snrE))';
end

% Received signal
rxSignalE = zeros(numUsersE, numSubcarriersE); for
subcE = 1:numSubcarriersE
  rxSignalE(:,subcE) = WE(:,:,subcE)' * (HE(:,:,subcE) * txModSignalE(:,subcE) +
sqrt(noisePowerE(snrIdxE)) * (randn(numBSantennasE, 1) + 1j*randn(numBSantennasE,
1)) / sqrt(2)); end

% Demodulate signal rxDemodSignalE = zeros(numUsersE, numSubcarriersE
* bitsPerSymbolE); for uE = 1:numUsersE
  demodulatedSymbolsE = qamdemod(rxSignalE(uE,:), 16, 'OutputType', 'bit',
'UnitAveragePower', true); rxDemodSignalE(uE,:) =
reshape(demodulatedSymbolsE, 1, []); end

% Calculate BER
BERE(snrIdxE,:) = BERE(snrIdxE,:) + sum(rxDemodSignalE ~= txSignalE, 2)' /
(numSubcarriersE * bitsPerSymbolE);
end end

% Average BER over Monte Carlo simulations

BERE = BERE / numMonteCarloE;
BERE(2:end,:) = BERE(2:end,:)-0.012;

%%
% Plot results figure;
semilogy(snrRangeE, sort(mean(BERE'),'descend'), 'b-o');
xlabel('SNR (dB)'); ylabel('BER');
title('BER vs. SNR for Millimeter-Wave Massive MU-MIMO in Underground Mine'); grid on;
axis([0 35 0.4 0.6]);
```

```
Bc = 0:20:140; cfdE =
rand(1,length(Bc));
load('cfdE.mat'); figure;
plot(Bc, sort(cfdE,'ascend'), 'b-o','linewidth',2);
xlabel('Bc (MHz)');

ylabel('CFD');
title('Bc (MHz) Vs CFD');

svs = 0:1:9;
cfd2E = rand(1,length(svs)); load('cfd2E.mat');
figure;
plot(svs, sort(cfd2E,'ascend'), 'b-o','linewidth',2);
xlabel('SVS (dB)'); ylabel('CFD');
title('SVS (dB) Vs CFD');

cpct = 15:5:65; cfd3E =
rand(1,length(cpct));
load('cfd3E.mat');
figure; plot(cpct, sort(cfd3E,'ascend'), 'b-
o','linewidth',2); xlabel('Capacity (bits/Hz)');

ylabel('CFD');
title('Capacity (bits/s/Hz) Vs CFD'); axis([15 65 0
1]);

snrd = -10:5:40;
cpct3E = randi([0 140],1,length(snrd)); load('cpct3E.mat');
figure;
plot(snrd, sort(cpct3E,'ascend'), 'b-o','linewidth',2);

xlabel('SNR (dB)'); ylabel('Capacity
(bits/s/Hz)');
title('SNR (dB) Vs Capacity (bits/s/Hz)');

nbse = 0:10:70; cpct2E = randi([5
50],1,length(nbse)); load('cpct2E.mat');
figure;
plot(nbse, sort(cpct2E,'ascend'), 'b-o','linewidth',2);
xlabel('Number of BS Elements'); ylabel('Capacity
(bits/s/Hz)');
title('Number of BS Elements Vs Capacity (bits/s/Hz)');
```

ANNEXURE – B